Article

Economic Dispatch of Microgrid Based on Load Prediction of Back Propagation Neural Network–Local Mean Decomposition–Long Short-Term Memory

Fengxia Xu [1,*], Xinyu Zhang [1], Xingming Ma [2], Xinyu Mao [2], Zhongda Lu [1], Lijing Wang [1] and Ling Zhu [1]

[1] School of Mechanical and Electrical Engineering, Qiqihar University, Qiqihar 161000, China; zhangxinyu871998@163.com (X.Z.); luzhongda@163.com (Z.L.); 02926@qqhru.edu.cn (L.W.); 02652@qqhru.edu.cn (L.Z.)

[2] State Grid Heilongjiang Provincial Electric Power Co., Ltd., Daqing Power Supply Company, Daqing 163458, China; mxm200x@126.com (X.M.); 2020911238@qqhru.edu.cn (X.M.)

* Correspondence: 01541@qqhru.edu.cn

Abstract: To plan the work of power generation equipment, it is necessary to ensure that the power supply is sufficient and to achieve the minimum cost to ensure the safety and economy of the microgrid. Based on back propagation neural network–local mean decomposition–long short-term memory (BPNN–LMD–LSTM) load prediction, the design is based on a fixed-time consistency algorithm with random delay to predict the economic dispatch of microgrids. Firstly, the initial power load prediction sequence is obtained by continuous training of the back propagation neural network (BPNN); the residual sequence with other influencing factors is decomposed by local mean decomposition (LMD); and the long short-term memory neural network (LSTM) is used to predict the output prediction residual sequence, and the final short-term power load prediction is obtained. Based on predicting load, the fixed-time consistency algorithm with random delay is used to add supply and demand balance constraints to optimize the power distribution of the power generation units of the distributed microgrid and reduce the power generation cost of the microgrid. The results show that the prediction model has better prediction accuracy, and the scheduling algorithm based on the prediction model has a faster convergence rate to reach the lowest power generation cost.

Keywords: BPNN–LMD–LSTM; load forecasting; stochastic latency; fixed-time consistency; microgrid

1. Introduction

Electric energy is an important material basis for human survival and development [1], and accurate prediction of electric energy consumption helps ensure the safe and stable operation of the power grid. Predicting short-term electricity loads within 1 week [2] has attracted the attention of researchers because of its important role in energy conservation. Methods based on machine learning and deep learning have been widely used in a variety of disciplines related to short-term load forecasting problems. For example, the back propagation neural network (BPNN) short-term load prediction algorithm is used in Ref. [3] to improve the convergence speed and accuracy. In Ref. [4], unknown nonlinear systems are identified, and a reliable FD threshold is found. A single method (classical method or ARTIFICIAL method) provides only a simple mathematical expression, which is not enough to describe the complete dependencies of the load sequence [5]. In Ref. [6], weather data and humidity data are entered into the BPNN model for power load forecasting. In Ref. [7], the relationship between daily average temperature, daily maximum temperature, daily minimum temperature, and short-term power load data is theoretically proved; an improved BPNN model is proposed to predict power load data, and a batch processing method is used to improve the convergence performance of the BPNN model. Due to the strong approximation ability of BPNN, it is widely used in the field of prediction. In

Ref. [8], a hybrid model of empirical mode decomposition (EMD) and LSTM is proposed. It uses the EMD algorithm to decompose the historical power data into several eigenmodal functions (IMFs) and trend components; it then uses short-term memory (STM) to predict the IMFs predicted values and finally adds up all the IMFs predicted values to obtain the final prediction results. The above literature considers the load forecasting problem, but the fundamental problem of the microgrid concerns the economic dispatch problem of the microgrid under the condition of solving the constraint of supply and demand balance.

As a small power generation and distribution system, the microgrid can better plan and operate its internal load prediction, and the power generation and energy storage equipment in the microgrid are regarded as multiple intelligent body nodes, and the functions of economic operation regulation and control of the microgrid can be realized through communication and exchange of information between nodes. The economic dispatch of the microgrid based on predicting the load can effectively reduce the decision-making time of the economic dispatch, thereby allocating the optimal power of the microgrid and reducing the cost of microgrid power generation. Additionally, combined with the plug-and-play characteristics of the distributed island microgrid, it is convenient to carry out follow-up inspection and maintenance of the microgrid power generation unit. Therefore, in Ref. [9], aiming at the shortcomings of the traditional centralized hierarchical control strategy, such as the single point of failure, a distributed hierarchical control framework of the microgrid is proposed. In Ref. [10], a distributed event-triggered secondary control method is proposed for the economic dispatch and frequency recovery control problems of sag-controlled AC microgrids. This control strategy ensures economic dispatch and frequency recovery control while bridging the time gap between AC microgrids and reducing the operation cost. The literature [11] proposes a consistent algorithm scheduling scheme under droop control, which realizes the fully distributed economic dispatch of microgrids that does not rely on the central processor, but their convergence speed is usually slow. The authors in Ref. [12] investigated the event-based finite-time consensus problems for second-order multi-agent systems with input delay. In Ref. [13], a finite-time economic scheduling algorithm that satisfies the supply demand balance and relies on the initial state of the incremental cost of distributed generator sets is considered. In Ref. [14], to achieve the control objective under the given constraints, the distributed control algorithms are designed for the second leader group and followers, in which the backstepping, distributed estimation, and adaptive gain design techniques are employed. The literature [15–18] proposes a time uniform delay problem based on micro-increment consistency to solve the economic scheduling problem. The authors in Ref. [19] investigated the effect of convergence velocity on the economic scheduling of the system without dependence on the fixed-time consistency of the initial state. In Ref. [20], a robust collaborative consensus algorithm for economic scheduling in a non-ideal communication environment is proposed. Huang et al. added a time-varying delay model to the distributed algorithm, so that the agent generators could use the delay information to achieve synergy [21]. In Ref. [22], the problems of frequency regulation and load economic dispatch are solved in the secondary control microgrid when the economic indicators meet the national standards. The secondary control proposed in Ref. [23] achieves economic generation control and distributed voltage control based on distributed consensus, by reducing the gap between traditional secondary control and tertiary control, and integrating traditional secondary control and tertiary control into one control layer. In Ref. [24], a secondary control (DMPSC) method based on distributed model prediction is proposed, which effectively meets the control requirements for microgrid systems. Considering the influence of delay, the literature [25] proposes a consensus-based distributed economic scheduling control algorithm. The literature [26] proposes a consensus algorithm to solve the economic scheduling problem under the influence of random delay, which can always meet the balance between supply and demand. The economic dispatch problem with supply and demand balance constraints is considered separately in the above literature, but it does not consider predicting the power load of the microgrid,

and the system will have a time delay problem due to the limited communication channel resources in the microgrid, resulting in the stability of the system being affected.

Therefore, a fixed-time consistency algorithm with random delay is proposed for load prediction based on a microgrid. Considering the factors of temperature, weather, and holidays affecting the electricity consumption of residents, a hybrid model of BPNN, LMD, and LSTM is proposed to predict the load power of the microgrid. Based on the forecast load, under the constraint of the supply and demand balance of the distributed microgrid, the fixed-time consistency algorithm with random delay is used to optimize the power distribution of the power generation unit of the distributed microgrid, reduce the power generation cost of the microgrid, and optimize the economic dispatch of the microgrid.

The remainder of this article is as follows. Section 2 describes the general framework for the economic dispatch of microgrid models based on load forecasting. Section 3 describes the microgrid load forecasting model and the resulting test. Section 4 introduces the economic dispatch forecasting method of the microgrid. Section 5 is the experimental simulation. Section 6 is a summary of the full text.

Based on the above analysis, the main contributions of this paper are summarized as follows:

(1)　In this paper, economic scheduling is proposed based on BP neural network, local mean decomposition, and long short-term memory network combined with load demand forecasting. The control mode adopts a distributed method to implement, and each node communicates the information with neighboring nodes to solve local optimization problems and reach an agreement asymptotically.

(2)　Considering the balance of power requirements in the system, this paper designs a fixed-time consistency with random delay to achieve a slight increase rate consistency, so that the operating cost is the lowest standard to provide output power regulation of distributed generation.

(3)　The simulation model is compared with the control scheme based on the classical control algorithm.

2. The General Framework for Economic Scheduling of Load Forecasting

Because the power load in the microgrid is affected by a variety of factors, such as weather, electricity prices, time factors, random factors, etc., the above factors are divided into major and secondary influencing factors, and all the data are entered into the BPNN model through data refinement for prediction. Since the residual value between the predicted value of the BPNN model and the actual value is generated, the LMD–LSTM model is established to predict the residual value, and the predicted value of the BPNN model is added to obtain the final prediction load. Based on the BPNN–LMD–LSTM model, the short-term load forecast establishes the supply and demand balance constraint, and the slight increase rate of each power generation unit is calculated by using the Lagrange multiplier method. Moreover, through the principle of micro-increment rate consistency, considering the time delay problem, a fixed-time consistency algorithm with random delay is proposed for microgrid power distribution, thereby predicting the power generation cost of the microgrid. The economic dispatch process based on microgrid load forecasting is shown in Figure 1.
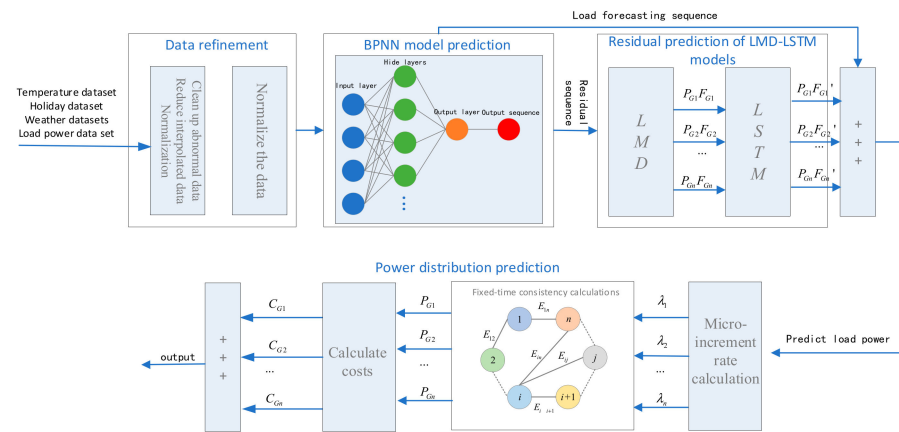
Figure 1. Schematic diagram of the economic dispatch framework for short-term load forecasting.

3. Microgrid Load Model Prediction and Result Testing

3.1. BPNN Model Prediction

BPNN has powerful computational power and complex mapping capabilities, enabling adaptive training of a large number of unstructured, imprecise laws. BPNN is used to make predictions with strong approximation capabilities. The raw data are used as input, divided into training sets and prediction sets, and a four-layer network structure of input layer, implicit layer, and output layer is constructed.

The initial weight is set to ω_{ij}, the number of hidden nodes in the hidden layer of the network is l, the activation function is f, and the model uses a gradient descent algorithm to supervise the training. When the prediction accuracy of the model is less than a certain error, the prediction set is entered into the network to calculate the load forecast sequence for the next 7 days. P_e is the residual sequence, that is, the difference between the predicted power load series and the actual power load value. Figure 2 shows the BPNN forecast flowchart.
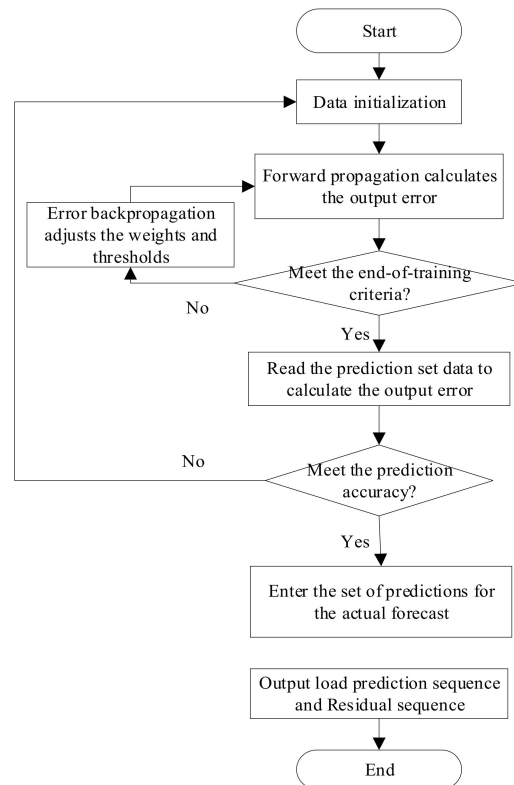

Figure 2. Schematic diagram of the economic dispatch framework for short-term load forecasting.

Since the BPNN model cannot effectively take into account the deviation caused by various factors, the residual difference between the predicted value and the actual value will be generated, so the LMD–LSTM model is established to predict the residual of the load power.

3.2. BPNN Model Prediction

LMD decomposition: Enter the residual sequence into the LMD decomposition to obtain the *n*-group product function *PF*, LMD decomposition flowchart, as shown in Figure 3.
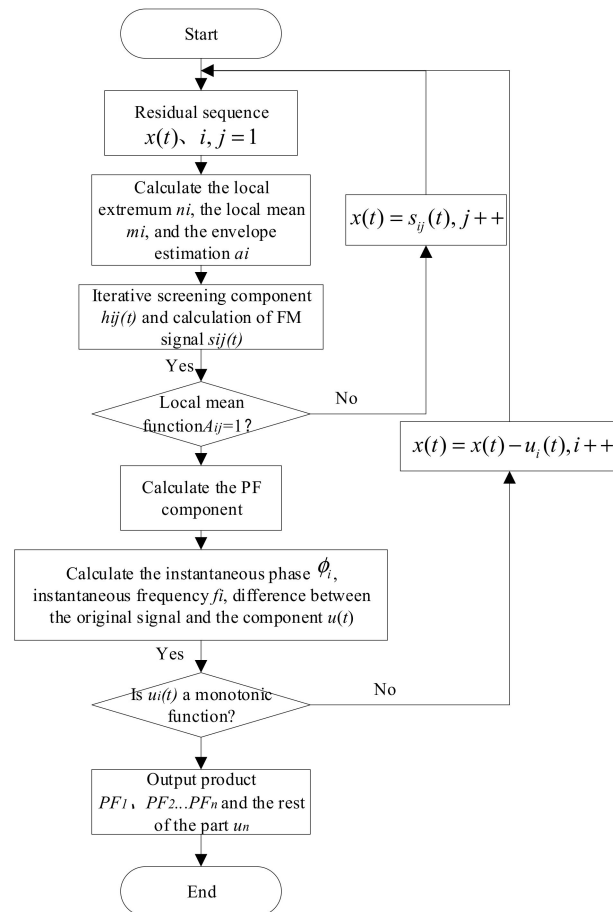

Figure 3. Flowchart of the LMD decomposition process.

Prediction of the LSTM model: First, the *PF* is normalized to the data, and its value range is planned in the range of [0, 1], and then used as input data for the LSTM neural network. The input data are processed by the input gate, the forgotten gate, and the output gate, which generates the retained information of the current storage unit o_t and the hidden state output h_t. h_t is output to the memory unit at the next moment and finally obtains the prediction $\{PF'_1, PF'_2, \cdots, PF'_n\}$ for each sequence of *PF* components. The prediction sequences are summed, so that the load prediction sequences obtained from the remaining forecast series P'_e and BPNN for the next 7 days are summed to obtain the accurate forecast value.

3.3. Data Refinement

When various data values of the original data are collected, problems such as equipment failure or missing data transmission will inevitably occur, resulting in outliers and missing values, which affect the prediction accuracy of the model. Therefore, outliers, missing interpolation, and data normalization are required for the original loaded data.

1. Handle outliers: Handle them according to the following formula:

$$Z = \frac{X - \mu}{\sigma} \tag{1}$$

where μ is the population average, X is the outlier, $X - \mu$ is the value that deviates from the mean, σ is the standard deviation, and Z is the difference between the original score and the population mean. By judging whether the absolute value of Z is greater than 2.2 by data Z. If it is greater than 2.2, delete the data row;

2. Handle missing values: Replace the missing values in the original data with *NaN* values, which correspond to the previous day's counterparts;

3. Data normalization: Weather data and holiday data are recorded in the text. Temperature data and power consumption data also have different ranges. The normalization process is used to facilitate the calculation of subsequent models. The minimum–maximum normalized method is used to convert temperature data and power consumption data into [0, 1] data. The calculation formula is as follows:

$$x_{norn} = \frac{x - x_{\min}}{x_{\max} - x_{\min}} \tag{2}$$

where x_{norn} is the normalized value and $x_{\min}$ and $x_{\max}$ are the minimum and maximum values in the dataset, respectively.

3.4. Microgrid Load Prediction Result Test

The difference between the load forecast series of P_b and P'_e for the next 7 days is summed to generate the power load forecast results for the next 7 days.

To test the prediction accuracy of the model, the mean absolute percentage error (MAPE), the mean absolute error (MAE), and the root mean square error (RMSE) are used to evaluate the prediction results [27]. It is calculated as:

$$MAPE = \frac{1}{n} \sum_{i=1}^{n} \frac{|\hat{y}_i - y_i|}{y_i} \times 100\% \tag{3}$$

$$MSE = \frac{1}{n} \sum_{i=1}^{n} (\hat{y}_i - y_i)^2 \tag{4}$$

$$RMSE = \sqrt{\frac{1}{n} \sum_{i=1}^{n} (\hat{y}_i - y_i)^2} \tag{5}$$

where $\hat{y}_i$ is the predicted value; y_i is the true value; and n is the number of predicted points. When the prediction accuracy is not ideal, the parameters of the BPNN model and the LMD–LSTM model need to be adjusted [19].

4. Economic Dispatching Method of Microgrid

4.1. Fixed-Time Consistency with Random Delay

Design a fixed-time distributed economic scheduling algorithm with random delay and combine it with a consistency algorithm. Considering the signal transmission speed, the system introduces a random delay effect. The random variable $\delta(t)$ is defined as follows:

$$\delta(t) = \begin{cases} 0 & \text{There is a delay in communication} \\ 1 & \text{There is no delay in communication} \end{cases} \tag{6}$$

where $\delta(t)$ is a Markov chain that satisfies the following exponential distribution transformations.

$$\begin{cases} P(\delta(t) = 1) = E\{\delta(t)\} = \bar{\delta} \\ P(\delta(t) = 0) = 1 - E\{\delta(t)\} = 1 - \bar{\delta} \end{cases} \tag{7}$$

where $P(\delta(t) = 1)$ represents the probability that no delay event will occur, and $P(\delta(t) = 0)$ represents the probability of a delay event occurring.

The expression for a fixed-time consistency algorithm with random delay is:

$$
\begin{aligned}
\dot{x}_i(t) = 2c\delta(t) \cdot \Big(&\sum_{j \in N_i} E_{ij} sig^{\alpha_{ij}}(x_j(t) - x_i(t)) + \sum_{j \in N_i} E_{ij} sig^{\beta_{ij}}(x_j(t) - x_i(t)) \Big) + 2c(1 - \delta(t)) \cdot \\
\Big(&\sum_{j \in Ni} E_{ij} sig^{\alpha_{ij}}(x_j(t - \tau) - x_i(t - \tau)) + \sum_{j \in N_i} E_{ij} sig^{\beta_{ij}}(x_j(t - \tau) - x_i(t - \tau)) \Big)
\end{aligned}
\tag{8}
$$

In Equation (10), $x_i(t)$ is an agent and a distributed power source of the microgrid, $x_j(t)$ is the state variable of the neighbor node, E_{ij} is the weight between the neighbor state variables, and $c > 0$ is the gain constant, which is used to adjust the convergence speed of the algorithm and satisfies any generator set: $\alpha_{ij} = \alpha_{ji}, \beta_{ij} = \beta_{ji}, \alpha_{ij} \in (0,1), \beta_{ij} \in (1, \infty)$. $sig^{\alpha}(s) = sign(s)|s|^{\alpha}$, where $sign(s)$ represents the symbolic function, $|s|$ represents the absolute value of the real number s, and τ is the time delay of the system.

4.2. Economic Dispatching of Microgrid Based on Load Forecasting

In the power allocation and cost calculation, assuming that the microgrid has N intelligent bodies, including wind power generation, photovoltaic power generation, micro gas turbines, fuel cells with four different types of power generation units, if one wants to make the microgrid intelligent system economically able to operate, first of all, the cost function model of each power generation unit is established, and the power generation cost function $C_i(P_{Gi})$ of each generator set can generally be approximately expressed by the quadratic function. The specific form is as follows:

In the power allocation and cost calculation, assuming that the microgrid has N intelligent bodies, including wind power generation, photovoltaic power generation, micro gas turbines, fuel cells with four different types of power generation units, if one wants to make the microgrid intelligent system economically able to operate, first of all, the cost function model of each power generation unit is established. The photovoltaic (PV) and wind energy conversion systems (WECS) are operated with maximum power point tracking control (MPPT). Hence, the renewable energy agent is considered a non-dispatchable agent and does not participate in economic scheduling. The power generation cost function $C_i(P_{Gi})$ of each generator set can generally be approximately expressed by the quadratic function. The specific form is as follows [28–30]:

$$
C_i(P_{Gi}) = \alpha_i + \beta_i P_{Gi} + \gamma_i P_{Gi}^2
\tag{9}
$$

where $\alpha_i, \beta_i, \gamma_i$ is the cost factor for each generator cost, and P_{Gi} is the output power of each generator set. Therefore, the total power generation cost function of the microgrid intelligent system is as follows:

$$
C(P) = \sum_{i=1}^{N} C_i(P_{Gi})
\tag{10}
$$

According to the above method, the load PF is predicted, and the Lagrange multiplier method is used to solve the optimal solution problem with the constraint of supply and demand balance. The Lagrange equation can be constructed according to Equation (10):

$$
L(P, \lambda) = \sum_{i=1}^{n} C_i(P_{Gi}) + \lambda \Big(PF - \sum_{i=1}^{n} P_{Gi} \Big)
\tag{11}
$$

The micro-increment rate $\lambda_i(P_{Gi})$ of the i-th generator set can be defined by the first-order optimization conditions as

$$
\lambda_i(P_{Gi}) = \frac{\partial C_i(P_{Gi})}{\partial P_{Gi}} = 2\gamma_i P_{Gi} + \beta_i
\tag{12}
$$

The generator set satisfies the constraints of supply and demand balance, and the mathematical model of smart grid economic dispatch known to contain equation constraints is

$$\min \sum_{i=1}^{n} C_i(P_{Gi})$$
$$s.t. \sum_{i=1}^{n} P_{Gi} = PF \tag{13}$$

Considering that there is no need to know the global information in the microgrid, the consensus algorithm is used for the economic dispatch of the microgrid. The slight increase rate of the generator set needs to be satisfied (12). Select the micro-increment consistency variable for each generator set, so the economic scheduling algorithm for considering the power supply and demand balance constraints is

$$\dot{\lambda}_i(t) = 2c\delta(t) \cdot \left(\sum_{j \in N_i} E_{ij} sig^{\alpha_{ij}}(\lambda_j(t) - \lambda_i(t)) + \sum_{j \in N_i} E_{ij} sig^{\beta_{ij}}(\lambda_j(t) - \lambda_i(t)) \right) + 2c(1 - \delta(t)) \cdot$$
$$\left(\sum_{j \in Ni} E_{ij} sig^{\alpha_{ij}}(\lambda_j(t-\tau) - \lambda_i(t-\tau)) + \sum_{j \in N_i} E_{ij} sig^{\beta_{ij}}(\lambda_j(t-\tau) - \lambda_i(t-\tau)) \right) \tag{14}$$

In Equation (13), $\lambda_i(t)$ is the slight increment rate of the *i*-th generator set, that is, the incremental cost.

5. Results

This section includes system configuration, datasets, evaluation metrics, experimental results from several traditional machine-learning and deep-learning models tested on the original dataset, and comparisons with other basic models.

5.1. Economic Dispatching of Microgrid Based on Load Forecasting

The proposed BPNN–LMD–LSTM model was validated using the dataset in the UCI knowledge base. The model was trained using a core I7 processor and 16GB of RAM. The experiment was performed in Python3Keras, which was later implemented using TensorFlow from the Adam optimizer.

5.2. Dataset

Consider that the power load data are affected by factors such as temperature, weather, holidays, and so on. Raw data are designed as time series data with multiple variables. The structure is shown in Figure 4.
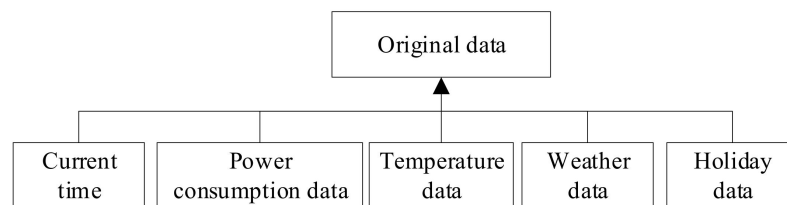

Figure 4. Flowchart of the LMD decomposition process.

Depending on the data refinement method, weather data and holiday data are converted to [0, 1] data based on their unique properties. Table 1 shows the quantitative processing table of weather attribute characteristic values, and Table 2 is the quantitative processing table of holiday characteristic values.

Table 1. Quantitative treatment table of weather attribute eigenvalue.

Weather Attributes	Value
Sunny	1
Cloudy	0.9
Overcast	0.8
Light rain	0.7
Moderate rain	0.6
Rainstorm	0.5
Sleet	0.4
Light snow	0.3
Moderate snow	0.2
Heavy snow	0.1
Heavy snowfall	0

Table 2. Quantitative treatment table of holiday eigenvalue.

Holiday Attributes	Value
Workdays	1
Weekends	0.5
Holidays	0

Short-term power loads are used to guide various plans for the microgrid in a day, including daily generation, daily dispatch, and daily power supply. The data come from the urban electricity load data of a city for 365 days from 1 January 2021 to 1 January 2022.

The data consist of 365-time-series data with six variables. These variables include daily maximum temperature values, daily average temperature values, minimum daily temperature values, weather impact factor values, power load values, and holiday impact factor values.

The first 358 pieces of data are entered into the prediction model, and the last 7 pieces of data are compared with the prediction data output by the prediction model to obtain the final experimental results. Data change curves for the datasets are shown in Figure 5.

(a)   (b)
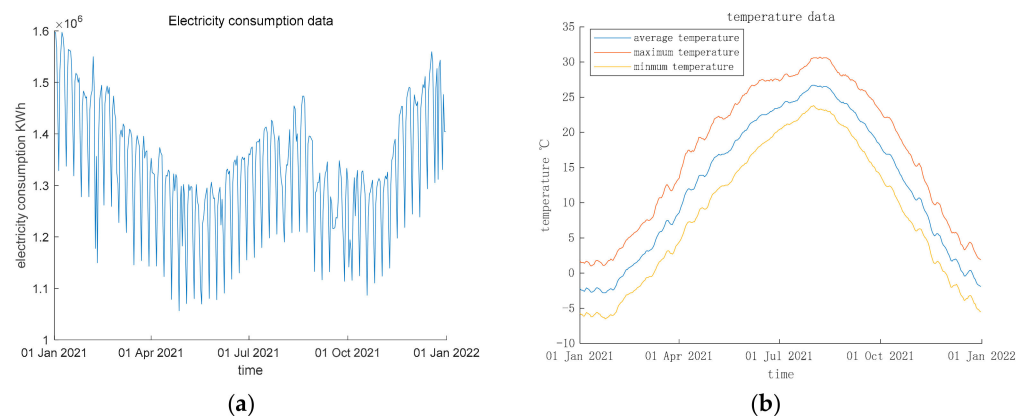
Figure 5. Load and temperature change in 2021. (**a**) Urban daily load change curve in 2021; (**b**) Temperature change curve of a city in 2021.

Holiday attribute D_t, temperature attribute T_t, and weather attribute W_t are used as the main influencing factors affecting the power load and input to BPNN. Use the standardized method to convert D_t, T_t, and W_t to a value between [0, 1].

5.3. BPNN Predicts Load Data

As can be seen from the above, the input variable of BPNN is D_t, T_t, and W_t output as the power load forecast value. A BPNN model with multiple input single output

hidden layers of 2 and hidden neurons (5, 13) is established. Use the "tanh" function as an activation function for neurons. The first 358 pieces of the above input data are used as the training set, and the mean squared error (MSE) is used as the loss function. The learning step η is 0.01, and the maximum number of cycles is $n = 10{,}000$. The weights of the hidden layer are trained using gradient descent.

After the training is completed, the input data D_t, T_t, and W_t of the first 358 days and the verification data of the next 7 days are used as the inputs of the BPNN model, and the prediction value Y_{btrain} of the training set and the prediction value Y_b of the prediction set are obtained. The residuals of the training set prediction are then calculated: $Y_e = Y - Y_{btrain}$. The prediction results and residual sequences of the BPNN model are shown in Figure 6.
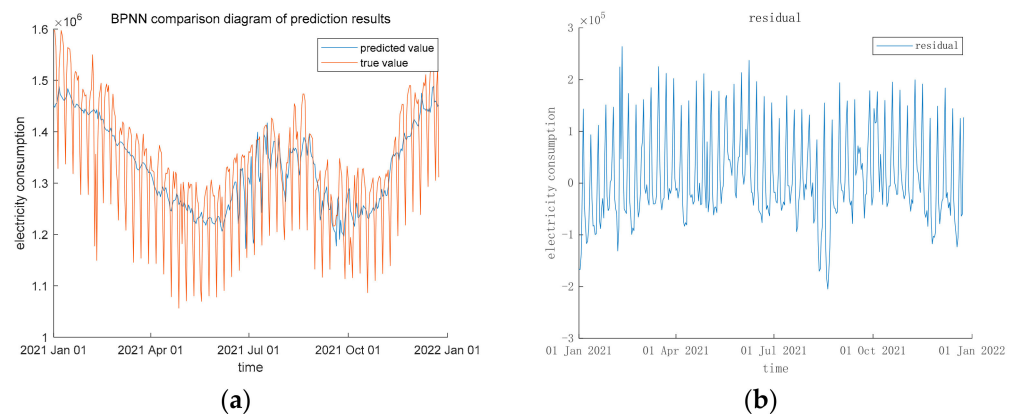
Figure 6. BPNN prediction result. (**a**) BPNN prediction result plot of raw data; (**b**) Residual sequence.

5.4. LMD–LSTM Residual Prediction

The residual sequence in Figure 6 is decomposed with LMD to obtain a component $PF_1 \sim PF_4$ of the product function that reflects the different characteristics of the electrical load of other influencing factors.

The product function components $PF_1 \sim PF_4$ are then fed into the LSTM model for training, and the predicted sequence $PF'_1 \sim PF'_4$ is obtained over the next 7 days. Finally, the residual prediction sequence Y' is obtained by adding $PF'_1 \sim PF'_4$. The training method of the LSTM model is as follows: the 358 component data are split into 322 prediction sequences of length 37, normalized, and merged into 322×37 matrices, i.e.:

$$
\begin{bmatrix}
PF_{n\_0} & \cdots & PF_{n\_36} \\
\vdots & \ddots & \vdots \\
PF_{n\_321} & \cdots & PF_{n\_357}
\end{bmatrix}
\tag{15}
$$

Among them, the first 30 columns of each piece of data are used as inputs to the LSTM model, and the last 7 columns are used as the output of the model. The model training uses the absolute mean error (MAE) as the loss function and the adaptive torque estimation method as the optimization algorithm. After the training is completed, obtain the forecast value PF for the next 7 days from 25 December 2021. Figure 7 shows the residual prediction results and PF component plots of the LMD–LSTM model.

Taking the prediction of a 7-day microgrid load as an example, BPNN–LMD–LSTM is used to predict the sum of load PFs, as shown in Figure 8. Among them, the forecast load on 25 December 2021 $PF = 1.57 \times 10^6$, the forecast load on 26 December 2021 $PF = 1.565 \times 10^6$, the forecast load on 27 December 2021 $PF = 1.485 \times 10^6$, the forecast load on 28 December 2021 $PF = 1.329 \times 10^6$, the forecast load on 29 December 2021 $PF = 1.528 \times 10^6$, the forecast load on 30 December 2021 $PF = 1.462 \times 10^6$, and the forecast load $PF = 1.463 \times 10^6$ on 31 December 2021.
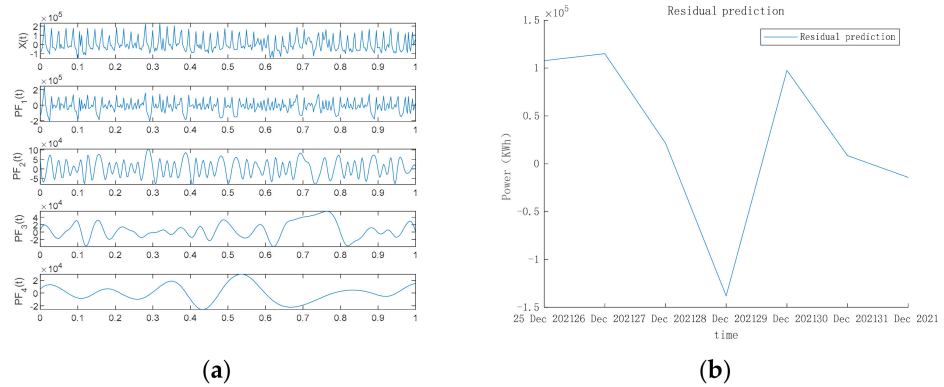
(**a**)   (**b**)

Figure 7. Output and residual prediction. (**a**) Each PF of the LSTM output; (**b**) Residual prediction.
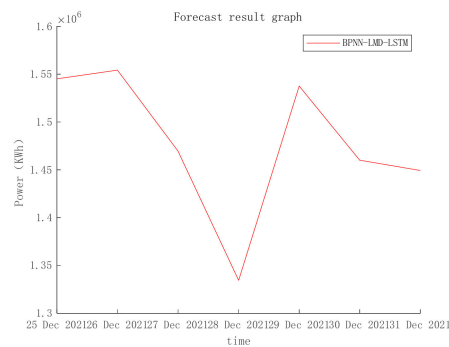

Figure 8. Sum of PF.

5.5. Economic Dispatching of Microgrid

Assuming that the microgrid has *N* agents, of which the smarts include four different types of power generation units—wind power generation, photovoltaic power generation, micro gas turbines, and fuel cells—the power generation unit communication topology diagram of the distributed island microgrid is simplified, as shown in Figure 9.
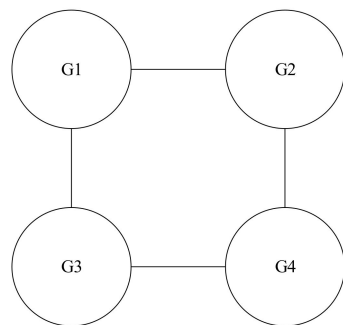

Figure 9. Power generation unit communication topology.

The cost function parameters and output power constraints are shown in Table 3.

Table 3. Parameters of power generations.

Power Generations	γ_i	β_i	P_i^m	P_i^M
G1	0.096	1.22	50	200
G2	0.072	3.41	50	200
G3	0.105	2.53	20	140
G4	0.082	4.02	20	60

Therefore, the Laplace matrix and adjacency matrix that simplify its communication topology are

$$A = \begin{bmatrix} 0 & 1 & 1 & 0 \\ 1 & 0 & 0 & 1 \\ 1 & 0 & 0 & 1 \\ 0 & 1 & 1 & 0 \end{bmatrix}; \ L = \begin{bmatrix} 2 & -1 & -1 & 0 \\ -1 & 2 & 0 & -1 \\ -1 & 0 & 2 & -1 \\ 0 & -1 & -1 & 2 \end{bmatrix} \tag{16}$$

where it is assumed that the weight of the neighboring node in the adjacency matrix is 1.

Taking the forecast load $PF = 1.57 \times 10^6$ on 25 December 2021 as an example for microgrid economic dispatching, to reflect the randomness of the delay, the value of $\delta(t)$ representing each sampling time is added. Its mathematical expectation is the random probability of system communication without delay $\bar{\delta} = 0.8$. Figure 10 shows an error between the total output power and the required load. Figure 11 shows the output power distribution of each power generation; then, the system meets the supply and demand balance constraints to distribute power. The power distribution of the microgrid at the lowest cost is shown in Figure 12a, and the total cost of the output power of each power generation unit is shown in Figure 12b.
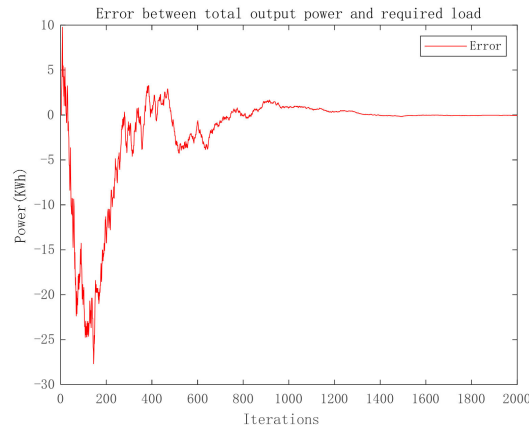

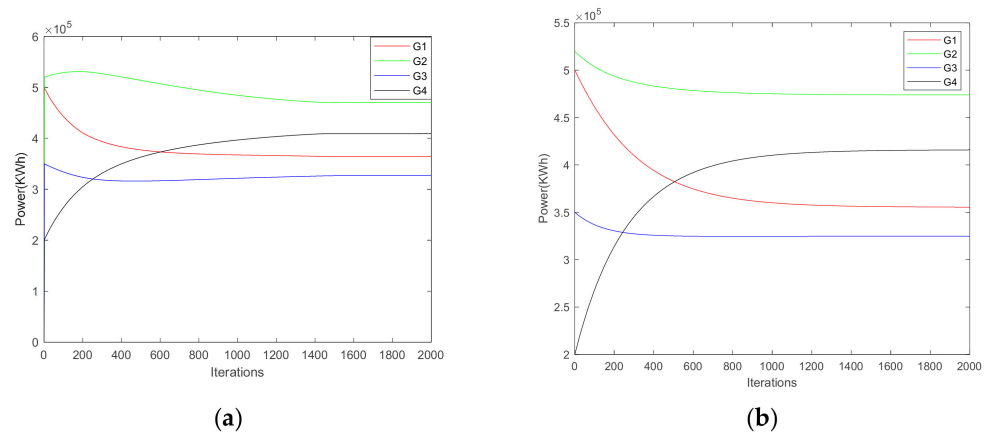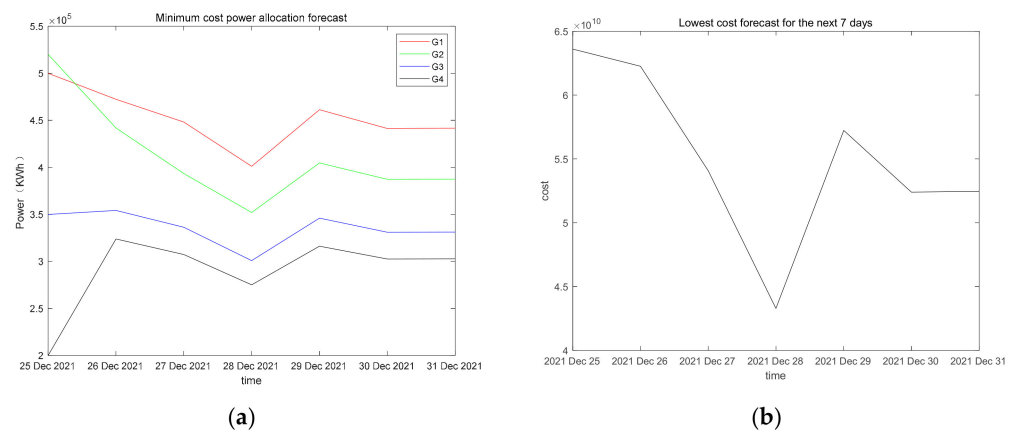**Figure 10.** The error between total output power and required load.

Figure 11. The output power distribution. (**a**) Fixed-time consistency of the power state at the random delay; (**b**) Classic consistency in the power state at the random delay.

Figure 12. The minimum power is its power distribution. (**a**) Microgrid power distribution at the lowest cost; (**b**) The lowest cost of microgrid output power for the next 7 days.

5.6. Evaluation Indicators

The prediction series Y_b and the prediction residuals series Y' are derived from the BPNN model and the LMD–LSTM model, respectively. Taking the prediction of the power load for the next 7 days as an example, $Y_b + Y'$ can be obtained.

To verify the accuracy of the prediction results of the proposed method, the same load data were predicted by using the BPNN model, the LSTM model, and the BPNN–EMD–LSTM model. A comparison of the four models is shown in Figure 13.
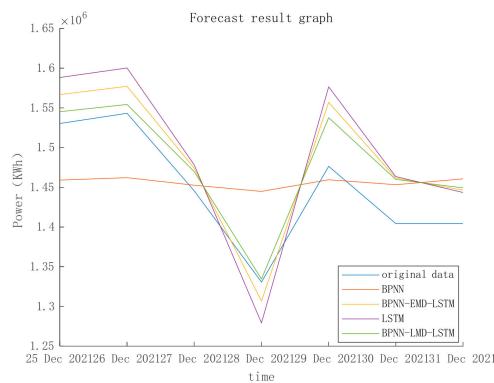
Figure 13. BPNN–LMD–LSTM hybrid model, BPNN, LSTM, and BPNN–EMD–LSTM comparison chart.

The error between the predicted value and the true value is then calculated by three methods: root mean square error (RMSE), mean absolute percentage error (MAPE), and mean absolute error (MAE). The predicted power load values and error rates of the four prediction models are shown in Table 4.

Table 4. Performance of different machine-learning and deep-learning models for UCI datasets.

Prediction Model	MAPE	MAE	RMSE
BPNN	3.70	5.38×10^4	1.96×10^4
LSTM	2.82	4.07×10^4	4.65×10^4
BPNN–EMD–LSTM	1.89	2.72×10^4	3.09×10^4
BPNN–LMD–LSTM	1.19	1.72×10^4	1.90×10^4

The following conclusions are drawn from Table 3. The three predictive evaluation indicators of the BPNN–LMD–LSTM combined model, MAPE, MAE, and RMSE had better

predictive effects than the single BPNN model, the LSTM model, and the BPNN–EMD–LSTM model. Although BPNN had better prediction accuracy on day 6, the BPNN–LMD–LSTM combined model had better predictions in the overall forecast.

To verify the rapidity of the convergence result of the scheduling algorithm, the same output power data are scheduled using the classical consistency algorithm. The slightly increasing rate pair with a random time delay is shown in Figure 14.
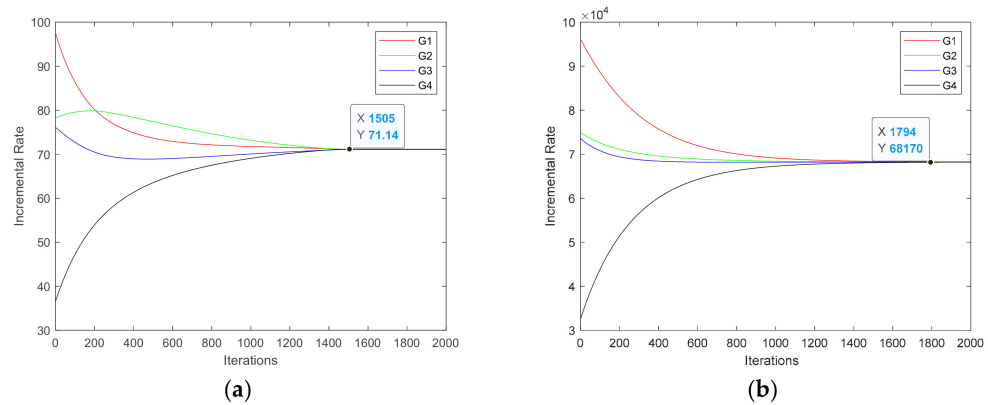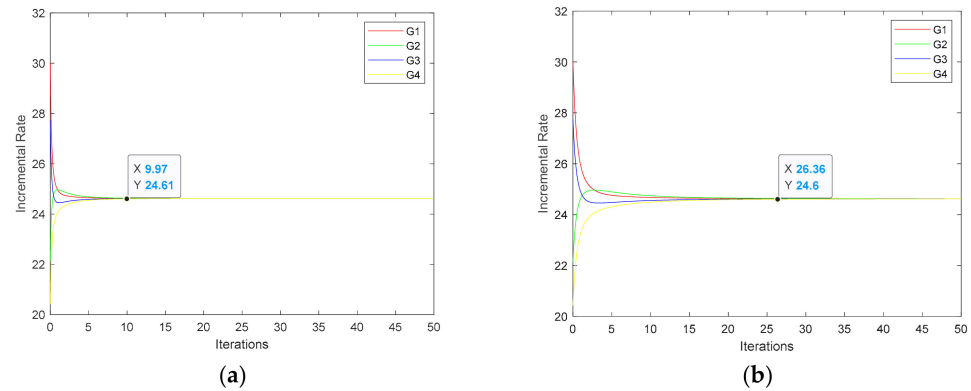

Figure 14. The rate of micro-increase. (**a**) The rate of micro-increase in fixed-time consistency at the random delay; (**b**) The rate of micro-increase in classical consistency at the random delay.

From the comparison of Figure 14a,b, it can be obtained that the classical time consistency with random delay converges at 1794 iterations, while the fixed-time consistency with random delay converges at 1505 iterations. It can be obtained that the algorithm proposed in this paper can solve the problem of slow convergence speed and improve the speed of dispatch while keeping the cost of microgrids to a minimum.

In Ref. [17], the K-step average consistency algorithm is used to economically dispatch the distributed microgrids and ensure the balance between supply and demand. Classical consensus algorithms are used in Ref. [26] for the economic dispatch of distributed microgrids. Figures 15 and 16, and Tables 5 and 6 are obtained by comparing the fixed-time consistency algorithm with the same data under the same conditions as Refs. [17,26], respectively, in the manuscript. Through experimental comparison, it is found that under the condition where the balance of supply and demand is met, the convergence time of the algorithm proposed in the manuscript is faster. Add experimental comparisons in Section 5.6 of the manuscript, listing the table below:
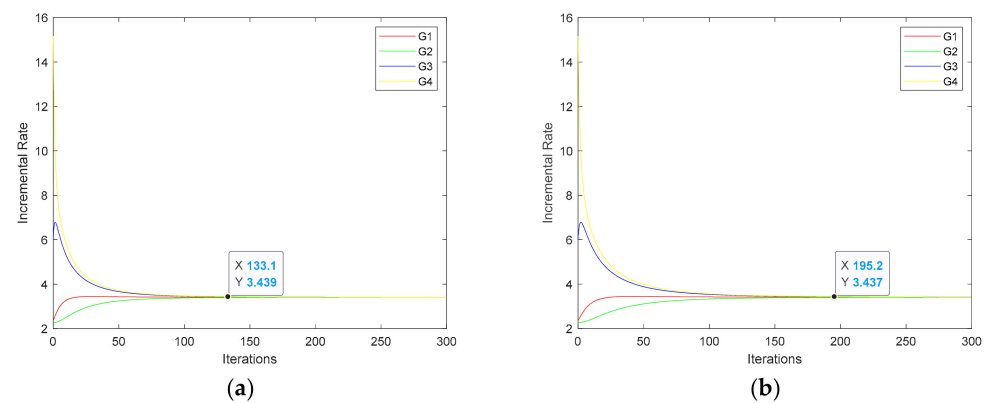
Figure 15. The rate of micro-increase. (**a**) The rate of micro-increase in fixed-time consistency at the random delay; (**b**) The rate of the K-step average consistency algorithm at the random delay.

Figure 16. The rate of micro-increase. (**a**) The rate of micro-increase in fixed-time consistency at the random delay; (**b**) The rate of the Classical consensus algorithm at the random delay.

Table 5. Demand load PD = 1500 MW, Total iteration time t = 300 s.

Algorithm	Convergence Time
Literature [17]	195.2 s
Fixed-time consistency	133.1 s

Table 6. Demand load PD = 500 MW, Total iteration time t = 50 s.

Algorithm	Convergence Time
Literature [26]	24.81 s
Fixed-time consistency	9.97 s

Through experimental comparison, it is found that the slight increase rate using the literature [17] algorithm converges at 195.2 s, and the micro-increase rate using the fixed-time consistency algorithm in the manuscript converges at 133.1 s; the micro-increment rate using the literature [26] algorithm converges at 24.81 s, and the micro-increase rate using the fixed-time consistency algorithm in the manuscript converges at 9.97 s.

5.7. IEEE 30-Bus

The optimal economic scheduling of IEEE 30-bus is verified by using a fixed-time consistency algorithm with random delay. The IEEE 30-bus test diagram is shown in Figure 17, and the communication topology is shown in Figure 18.

The parameters of the cost function are shown in Table 7, assuming that the requirements PD =295.36 MWh, $P_{G1}(0) = 133.36$ MWh, $P_{G2}(0) = 70$ MWh, $P_{G3}(0) = 40$ MWh, $P_{G4}(0) = 20$ MWh, $P_{G5}(0) = 15$ MWh, $P_{G6}(0) = 17$ MWh.

Table 7. Parameters of power generations in the IEEE 30-bus.

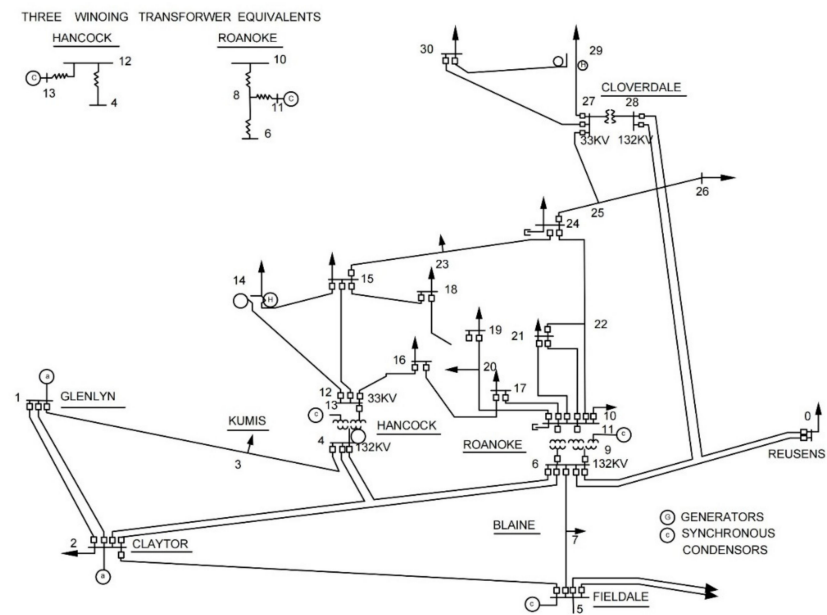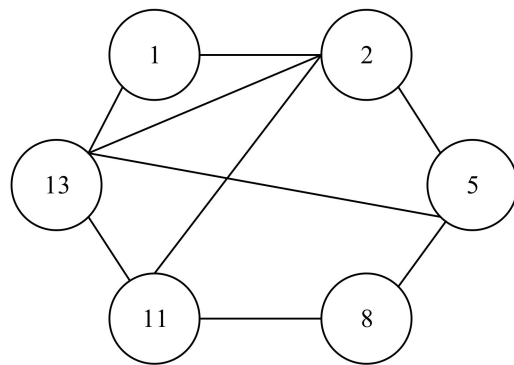| Unit (Generator No.)	α_i	β_i	γ_i	P_{min}	P_{max}
G1 (1)	0	2.00	0.00375	50	200
G2 (2)	0	1.75	0.01750	20	80
G3 (5)	0	1.00	0.06250	15	50
G4 (8)	0	3.25	0.00834	10	35
G5 (11)	0	3.00	0.02500	10	30
G6 (13)	0	3.00	0.02500	12	40

Figure 17. The IEEE 30-bus diagram.

Figure 18. The IEEE 30-bus communication topology.

The incremental cost of fixed-time consistency is shown in Figure 19, where the micro-increment rate converges after 704 iterations, and the individual micro-increment rates reach a consensus. The optimal economic dispatch is thus achieved, and the power distribution is $P_{G1}^* = 193.0615$ MWh, $P_{G2}^* = 48.5339$ MWh, $P_{G3}^* = 19.5968$ MWh, $P_{G4}^* = 12.0459$ MWh, $P_{G5}^* = 10.0892$ MWh, $P_{G6}^* = 12.0326$ MWh.
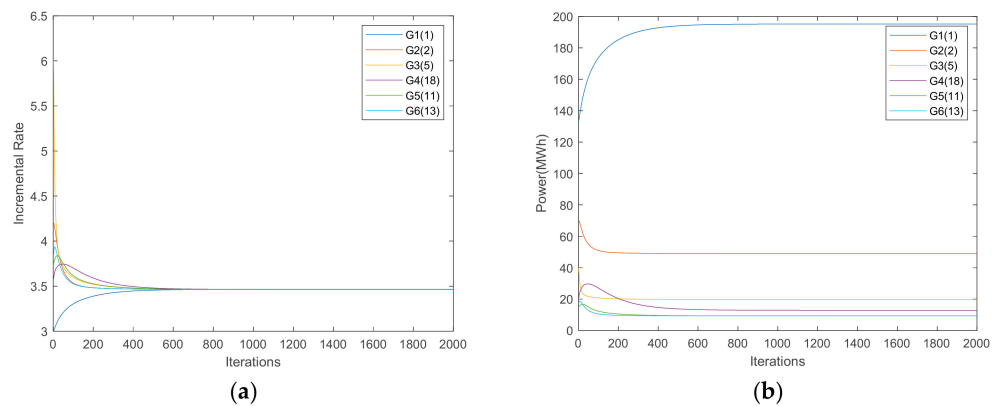

(**a**)

(**b**)

Figure 19. IEEE 30-bus test system. (**a**) The rate of micro-increase in fixed-time consistency at the random delay, (**b**) Fixed-time consistency of the power state at the random delay.

6. Conclusions

In this paper, an economic dispatching method based on the BPNN–LMD–LSTM model short-term microgrid load prediction is proposed. Experiments on the original dataset for evaluating the hybrid BPNN–LMD–LSTM model show that the error rate of MAE and RMSE is reduced by 2%, the influence of various external factors on the microgrid load data is fully explored, and the short-term microgrid load prediction of the city is more accurately completed. It also proposes that the fixed-time consistency algorithm with random delay improves the time for the system to calculate the economic dispatch result while obtaining the lowest economic cost, reduces the error of the calculation result, and effectively reduces the economic cost under the premise of ensuring the high-speed and stable operation of the microgrid system. This method better assists the relevant personnel of the microgrid work to make decisions, and to a certain extent, it is conducive to the depth perception of short-term microgrid load data, which has important economic value for the engineering application of the microgrid system and also provides a foundation for the construction and development of the smart grid.

Author Contributions: Conceptualization, F.X., X.Z. and Z.L.; Data curation, X.M. (Xinyu Mao); Formal analysis, X.Z. and L.W.; Funding acquisition, F.X.; Methodology, F.X. and X.Z.; Project administration, F.X.; Resources, Z.L. and L.Z.; Software, X.Z.; Supervision, X.M. (Xingming Ma) and X.M. (Xinyu Mao); Visualization, L.Z.; Writing—review & editing, F.X., X.Z., X.M. (Xingming Ma), X.M. (Xinyu Mao), Z.L., L.W. and L.Z. All authors have read and agreed to the published version of the manuscript.

Conflicts of Interest: The authors declare no conflict of interest.

References

1. Zhao, G.; Liu, Z.; He, Y.; Cao, H.; Guo, Y. Energy consumption in machining: Classification, prediction, and reduction strategy. *Energy* **2017**, *133*, 142–157. [CrossRef]
2. Liang, Y.; Niu, D.; Hong, W.C. Short term load forecasting based on feature extraction and improved general regression neural network model. *Energy* **2019**, *166*, 653–663. [CrossRef]
3. Luo, Y.; Cai, Y.; Qi, Y.; Huang, H. BP neural network short-term load forecasting algorithm based on maximum deviation similarity criterion. *Comput. Appl. Res.* **2018**, *36*, 1–8.
4. Ran, G.; Chen, H.; Li, C.; Ma, G.; Jiang, B. A Hybrid Design of Fault Detection for Nonlinear Systems Based on Dynamic Optimization. *IEEE Trans. Neural Netw. Learn. Syst.* **2022**, 1–11. [CrossRef]
5. Zhang, Y.; Guo, L.; Li, Q.; Li, J. Electricity consumption forecasting method based on MPSO-BP neural network model. In Proceedings of the 2016 4th International Conference on Electrical & Electronics Engineering and Computer Science (ICEEECS 2016), Jinan, China, 15–16 October 2016.
6. Liu, X.; Luo, D.S.; Yao, J.G.; Zhou, X. Short-term load forecasting based on load decomposition and hourly weather factors. *Power Syst. Technol.* **2009**, *33*, 94–100.
7. Zhao, D.; Ku, W.; Li, D.; Li, W.; Hua, G. Influence of Meteorological Factors on Short-term Load Prediction Accuracy of Power System. *Yunnan Electr. Power* **2017**, *45*, 49–52.
8. Dai, S.; Chen, Q.; Liu, Z.; Dai, H. Time series prediction based on EMD-LSTM model. *Sci. Eng.* **2020**, *37*, 265–270. [CrossRef]
9. Ullah, S.; Khan, L.; Sami, I.; Hafeez, G.; Albogamy, F.R. A Distributed Hierarchical Control Framework for Economic Dispatch and Frequency Regulation of Autonomous AC Microgrids. *Energies* **2021**, *14*, 8408. [CrossRef]
10. Li, Z.; Cheng, Z.; Liang, J.; Si, J.; Dong, L.; Li, S. Distributed Event-Triggered Secondary Control for Economic Dispatch and Frequency Restoration Control of Droop-Controlled AC Microgrids. *IEEE Trans. Sustain. Energy* **2020**, *11*, 1938–1950. [CrossRef]
11. Zheng, S.; Liao, K.; Yang, J.; He, Z. Droop-based consensus control scheme for economic dispatch in islanded microgrids. *IET Gener. Transm. Distrib.* **2020**, *14*, 4529–4538. [CrossRef]
12. Ran, G.; Liu, J.; Li, C.; Chen, L.; Li, D. Event-Based Finite-Time Consensus Control of Second-Order Delayed Multi-Agent Systems. *IEEE Trans. Circuits Syst. II Express Briefs* **2021**, *68*, 276–280. [CrossRef]
13. Yan, H.; Han, J.; Zhang, H.; Zhan, X. Adaptive Event-Triggered Predictive Control for Finite Time Microgrid. *IEEE Trans. Circuits Syst. I* **2020**, *67*, 1035–1044. [CrossRef]

14. Chen, L.; Mei, J.; Li, C.; Ma, G. Distributed Leader–Follower Affine Formation Maneuver Control for High-Order Multiagent Systems. *IEEE Trans. Autom. Control* **2020**, *65*, 4941–4948. [CrossRef]
15. Chen, G.; Li, Z. Consensus based distributed finite-time economic dispatch in smart grid with jointly connected topology. In Proceedings of the 2017 29th Chinese Control and Decision Conference (CCDC), Chongqing, China, 28–30 May 2017; pp. 7013–7018.
16. Zhao, C.; Duan, X.; Shi, Y. Analysis of Consensus-Based Economic Dispatch Algorithm under Time Delays. *IEEE Trans. Syst. Man Cybern. Syst.* **2020**, *50*, 2978–2988.
17. Zhang, Y.; Sun, Y.; Wu, X.; Sidorov, D.; Panasetsky, D. Economic Dispatch in Smart Grid Based on Fully Distributed Consensus Algorithm with Time Delay. In Proceedings of the 2018 37th Chinese Control Conference (CCC), Wuhan, China, 25–27 July 2018; pp. 2442–2446.
18. Wu, J.; Zhu, B.; Liong, Y.; He, Y. Research on the Influence of Communication Time-Delay on Multi-agent System Based Distributed Energy Dispatching Control Consensus. *IOP Conf. Ser. Earth Environ. Sci.* **2020**, *555*, 012091. [CrossRef]
19. Dong, Y.; Chen, J.; Cao, J. Fixed-time consensus of nonlinear multi-agent systems with stochastically switching topologies. *Int. J. Control* **2021**, 1–21. [CrossRef]
20. Xu, H.; Zhang, X.; Yu, T. Robust collaborative consensus algorithm for economic dispatch of non-ideal communication network. *Autom. Electr. Power Syst.* **2016**, *140*, 597–610.
21. Huang, B.; Liu, L.; Zhang, H.; Li, Y.; Sun, Q. Distributed Optimal Economic Dispatch for Microgrids Considering Communication Delays. *IEEE Trans. Syst. Man Cybern. Syst.* **2019**, *49*, 1634–1642. [CrossRef]
22. Ullah, S.; Khan, L.; Sami, I.; Ro, J.-S. Voltage/Frequency Regulation with Optimal Load Dispatch in Microgrids using SMC based Distributed Cooperative Control. *IEEE Access* **2022**, *10*, 64873–64889. [CrossRef]
23. Li, Z.; Zang, C.; Zeng, P.; Yu, H.; Li, S. Fully Distributed Hierarchical Control of Parallel Grid-Supporting Inverters in Islanded AC Microgrids. *IEEE Trans. Ind. Inform.* **2018**, *14*, 679–690. [CrossRef]
24. Mehmood, F.; Khan, B.; Ali, S.M.; Rossiter, J.A. Distributed model predictive based secondary control for economic production and frequency regulation of MG. *IET Control Theory Appl.* **2019**, *13*, 2948–2958. [CrossRef]
25. Gang, C.; Zhao, Z. Delay Effects on Consensus-Based Distributed Economic Dispatch Algorithm in Microgrid. *IEEE Trans. Power Syst.* **2017**, *33*, 602–612.
26. Yu, M.; Song, C.; Feng, S.; Tan, W. A consensus approach for economic dispatch problem in a microgrid with random delay effects. *Int. J. Electr. Power Energy Syst.* **2020**, *118*, 10579. [CrossRef]
27. Chai, T.; Draxler, R.R. Root mean square error (RMSE) or mean absolute error (MAE). *Geosci. Model Dev. Discuss.* **2014**, *7*, 1525–1534.
28. Xia, H.; Li, Q.; Xu, R.; Chen, T.; Wang, J.; Hassan, M.A.S.; Chen, M. Distributed Control Method for Economic Dispatch in Islanded Microgrids with Renewable Energy Sources. *IEEE Access* **2018**, *6*, 21802–21811. [CrossRef]
29. Yu, W.; Li, C.; Yu, X.; Wen, G.; Lü, J. Economic power dispatch in smart grids: A framework for distributed optimization and consensus dynamics. *Sci. China Inf. Sci.* **2018**, *61*, 012204. [CrossRef]
30. Zhang, Z.; Chow, M.-Y. Convergence Analysis of the Incremental Cost Consensus Algorithm under Different Communication Network Topologies in a Smart Grid. *IEEE Trans. Power Syst.* **2012**, *27*, 1761–1768. [CrossRef]